International Journal for Parasitology: Drugs and Drug Resistance 30 (2026) 100631

Contents lists available at ScienceDirect

International Journal for Parasitology: Drugs and Drug Resistance

journal homepage: www.elsevier.com/locate/ijpddr

Anti-cryptosporidial efficacy of tricyclic carbazole aminoalcohols in vitro and in vivo

Mingxiao Liu [a,b], Weisi Wang [c], Qi Zheng [c], Di Zhang [a], Dongqiang Wang [a], Chenchen Wang [a], Jigang Yin [a], Liping Duan [c,*], Guan Zhu [a,**]

[a] State Key Laboratory for Diagnosis and Treatment of Severe Zoonotic Infectious Diseases, Institute of Zoonosis, and College of Veterinary Medicine, Jilin University, Changchun, China
[b] College of Veterinary Medicine, Jilin Agricultural University, Changchun, China
[c] National Institute of Parasitic Diseases, Chinese Center for Disease Control and Prevention, Key Laboratory of Parasite and Vector Biology, Ministry of Health, WHO Collaborating Centre for Tropical Diseases, Shanghai, China

ARTICLE INFO

Keywords:
Cryptosporidium
Carbazole aminoalcohols
Antiparasitic drug discovery
In vitro efficacy
Mouse efficacy model
Selectivity index

ABSTRACT

Cryptosporidiosis is a major cause of diarrheal disease in humans and animals, yet there are no fully effective drugs, particularly for immunocompromised patients. Carbazole aminoalcohols (CAAs) are a relatively unexplored chemical class with reported broad-spectrum antiparasitic activities. Here, we systematically evaluated 36 CAA derivatives for anti-cryptosporidial efficacy. In vitro screening using a 44-h *Cryptosporidium parvum* infection assay identified eight compounds with low-micromolar EC_{50} values (1.53–6.86 μM). The three most potent hits (H1402 at 25 mg/kg/d, and YFM1 and YFM3 at 15 mg/kg/d) were selected for in vivo evaluation in a chronic *C. tyzzeri* mouse model. Daily oral treatment with these compounds for 7 days reduced fecal oocyst shedding by 55.9–59.1 % compared with a 247.5 % increase in vehicle controls ($P < 0.01$). Paromomycin at 1000 mg/kg/d, used as a positive control, produced an 84.2 % reduction. All three CAAs were generally well tolerated, with only minor weight loss observed in H1402-treated mice. Together, these results demonstrate that CAAs possess reproducible in vitro activity and significant in vivo efficacy against cryptosporidial infection, supporting their potential as lead scaffolds for anti-cryptosporidial drug development. Structural optimization to improve potency, selectivity, and pharmacokinetic properties is warranted to advance CAAs toward preclinical development.

1. Introduction

Cryptosporidium parvum is a globally distributed protozoan parasite and a leading cause of diarrheal disease in humans and animals. Its environmentally robust oocysts, which resist standard chlorination, are responsible for anthroponotic and zoonotic transmission through contaminated water and food (Wang et al., 2024b). Cryptosporidiosis is particularly severe in vulnerable populations, including infants, the elderly, transplant recipients, and individuals undergoing chemotherapy or living with HIV/AIDS, where infections can become chronic and life-threatening (Checkley et al., 2015). In low- and middle-income countries, *Cryptosporidium* ranks among the top etiologic agents of moderate-to-severe diarrhea in children under five, contributing to malnutrition, developmental stunting, and significant mortality (Kotloff et al., 2013; Levine et al., 2020). In livestock, especially the cattle and dairy industry, *C. parvum* is a major cause of neonatal calf diarrhea, leading to substantial economic losses worldwide (Roblin et al., 2023; Shaw et al., 2020).

Despite its public health and veterinary significance, treatment options remain limited. Nitazoxanide is the only drug currently approved for cryptosporidiosis in immunocompetent patients ≥1 year of age, but its clinical efficacy is incomplete and it fails in immunocompromised hosts (Khan and Witola, 2023; Love and Choy, 2021). These limitations have prompted intense efforts over the past decade to identify novel anti-cryptosporidial agents. Several promising leads from diverse chemical classes have demonstrated potent efficacy both in vitro and in animal models (Khan and Witola, 2023; Schneider et al., 2021).

In this study, we focused on a relatively unexplored chemical class,

* Corresponding author.
** Corresponding author.
E-mail addresses: duanlp@nipd.chinacdc.cn (L. Duan), cryptosporida@gmail.com (G. Zhu).

https://doi.org/10.1016/j.ijpddr.2026.100631
Received 30 September 2025; Received in revised form 25 December 2025; Accepted 2 January 2026
Available online 3 January 2026

carbazole aminoalcohols (CAAs), as potential anti-cryptosporidial agents. CAAs are characterized by a planar, nitrogen-containing tricyclic carbazole core linked to a chiral aminoalcohol moiety (Fig. 1A; also see Supplementary Fig. S1 and Table S1) (Molette et al., 2013; Smith et al., 2013). The electron-rich aromatic core and hydrogen-bonding side chain together confer unique physicochemical properties that are attractive for drug discovery. Previous studies have reported broad antiparasitic activities of selected CAAs, with low-micromolar in vitro efficacies against the protoscolices of *Echinococcus granulosus* and *E. multilocularis*, and the cercariae and adult worms of *Schistosoma japonicum*, as well as sub-micromolar in vitro activities against *Plasmodium falciparum* and *Trypanosoma brucei* (Cai et al., 2021; Dang et al., 2018; Liu et al., 2018; Molette et al., 2013; Wang et al., 2017a, 2017b).

Here, we systematically evaluated 36 CAA derivatives for their anti-

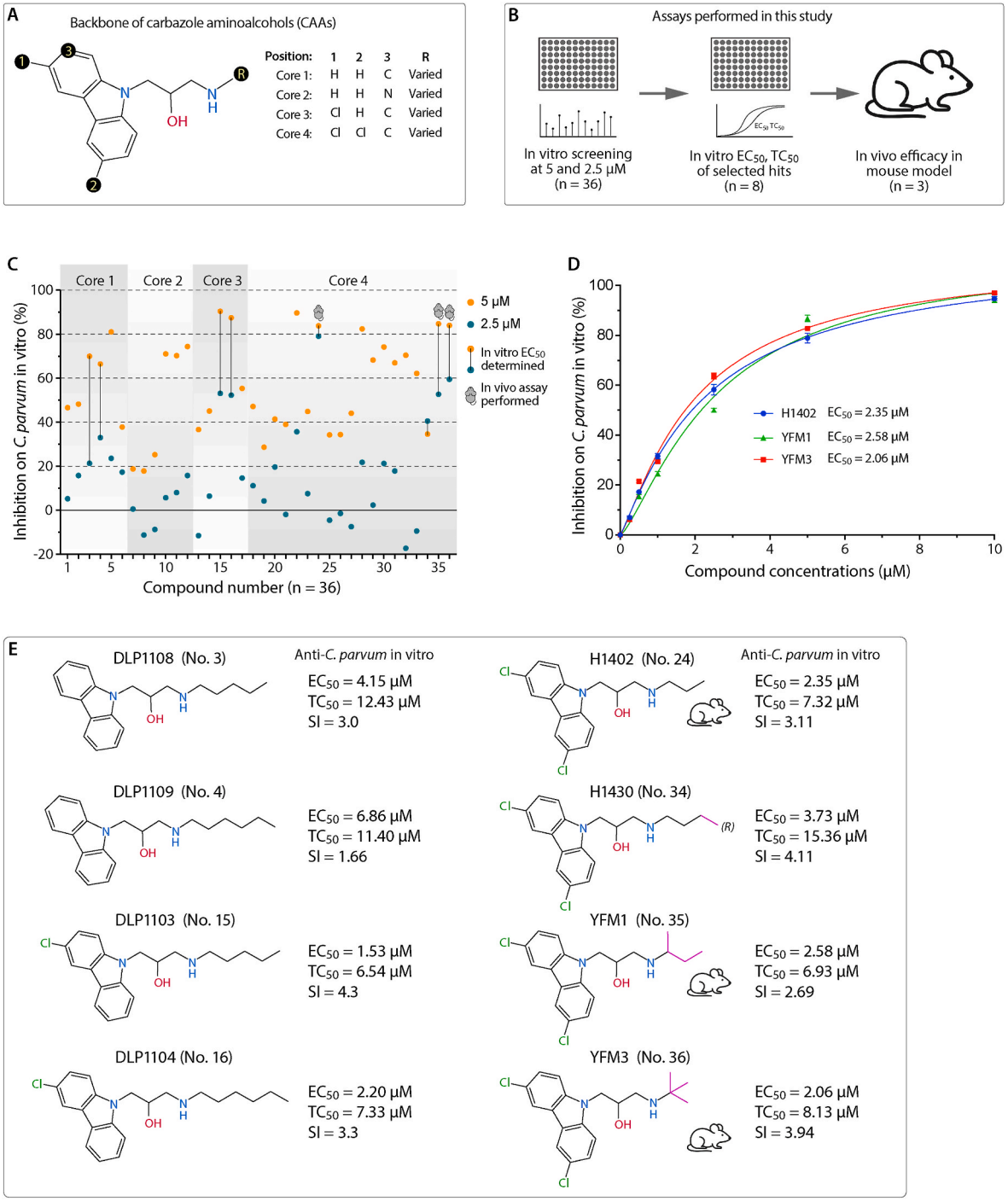

Fig. 1. In vitro screening and potency determination of carbazole aminoalcohols (CAAs) against *Cryptosporidium parvum*. (A) General chemical structure of carbazole aminoalcohols, showing the tricyclic carbazole core (cores 1–4) and the variable aminoalcohol side chains. **(B)** Workflow of the screening strategy used in this study: 36 CAA analogues were screened in vitro, eight hits were selected for dose–response analysis, and three top hits were subsequently evaluated in vivo. **(C)** Percent inhibition of parasite growth at 2.5 μM and 5 μM for all 36 CAAs, quantified by qRT-PCR in a 44-h infection assay. **(D)** Dose–response curves for the three selected hits showing EC_{50} values. Data represent means of three biological replicates, with technical duplicates per replicate. **(E)** Chemical structures of the eight most active analogues (core type and side chain indicated). In vitro efficacy (EC_{50} values), cytotoxicity on HCT-8 cells (TC_{50} values), and selectivity indices ($SI = TC_{50}/EC_{50}$) are provided for each compound.

cryptosporidial activity (Fig. 1B). Compounds with the highest in vitro potency were further assessed in a mouse model of chronic *C. tyzzeri* infection. We report that several tricyclic CAA analogues display low-micromolar efficacy in vitro and moderate but significant in vivo activity, supporting the potential of CAAs as lead scaffolds for future anti-cryptosporidial drug development.

2. Materials and Methods

2.1. Ethic statement

All animal experiments were performed in compliance with the *Guide for the Care and Use of Laboratory Animals* of the Ministry of Health of China and were approved by the Animal Welfare and Research Ethics Committee of the Institute of Zoonosis, Jilin University (AUP #2020-1Z-20 and #2024-IZ-00039). Bovine calves were used to propagate *C. parvum*, and mice were used for propagation of *C. tyzzeri* and for in vivo drug efficacy experiments.

2.2. Parasites materials

Two *Cryptosporidium* species were employed in this study. The *C. parvum* isolate (Gp60 subtype IIdA19G1), which was used for in vitro drug efficacy assays, was propagated in calves as described previously (Li et al., 2025; Wang et al., 2024b). The *C. tyzzeri* JLU01 strain, which was used for in vivo drug efficacy assays, was maintained in either KM or C57BL/6 mice that were given dexamethasone phosphate (DXP; 30 μg/mL) and tetracycline (TET; 50 μg/mL) in drinking water on alternating days (Liu et al., 2023). Oocysts were purified from feces by discontinuous sucrose/CsCl gradient centrifugation, suspended in PBS containing penicillin (200 U/mL) and streptomycin (0.2 mg/mL), and stored at 4 °C for no more than three months before use (Li et al., 2025; Liu et al., 2023; Wang et al., 2024a). Only oocyst batches with excystation rates exceeding 80 % were used in both in vitro and in vivo experiments. Prior to infection, oocysts were treated on ice with 10 % bleach for 5 min to inactivate potential contaminants, washed five to eight times with PBS. Bleached oocysts of *C. parvum* or *C. tyzzeri* were resuspended either in RPMI-1640 medium containing 10 % fetal bovine serum (complete cell culture medium) for in vitro assays or in PBS for animal inoculation.

2.3. Carbazole aminoalcohol compounds

Thirty-six carbazole aminoalcohol (CAA) derivatives were synthesized and purified by preparative HPLC to ≥98 % purity following previously published procedures (Dang et al., 2018; Liu et al., 2018; Wang et al., 2017a, 2017b). These compounds feature a tricyclic, nitrogen-containing carbazole core with different halogenation patterns (cores 1–4) and aminoalcohol side chains of varied length and branching (3–8 carbons) (Fig. 1A; Supplementary material, Supplementary Fig. S1 and Table S1). The structural diversity within this library allowed for evaluation of both electronic effects of core substitution and steric/hydrophobic effects of the side chains on anti-parasitic activity.

2.4. In vitro growth inhibition assay

Anti-cryptosporidial activity in vitro was measured using a 44-h growth inhibition assay with *C. parvum* infection of HCT-8 cells, and parasite burdens were quantified by qRT-PCR as previously described (Zhang and Zhu, 2015, 2020). HCT-8 cells were maintained in RPMI-1640 medium supplemented with 10 % fetal bovine serum (FBS), 50 U/mL penicillin, and 50 μg/mL streptomycin at 37 °C in a humidified incubator with 5 % CO_2. For assays, cells were seeded into flat-bottom 96-well plates and incubated overnight until reaching approximately 80 % confluence.

Oocysts of *C. parvum* were suspended in complete medium containing 0.15 % sodium taurocholate and added to each well at 2×10^4 oocysts/well by medium exchange to initiate infection. After a 3 h incubation at 37 °C to allow excystation and invasion, wells were washed once with RPMI-1640 medium to remove unexcysted oocysts and free sporozoites. Test compounds were then added at indicated final concentrations (5 and 2.5 μM in primary screens, and typically 0.3–10 μM in dose-responses) in complete medium containing 0.5 % DMSO. Infected cells were cultured for additional 41 h at 37 °C. Sodium taurocholate was absent in the culture medium during the 41 h drug treatment. Each plate included vehicle controls with 0.5 % DMSO alone. Primary screens were performed with three biological replicates at each concentration, whereas dose–response experiments used two replicates per concentration, with at least five replicates for the vehicle control group to allow reliable normalization.

At 44 h post-infection (hpi), plates were centrifuged briefly to secure cell monolayers, and the culture supernatants were discarded carefully (Zhang and Zhu, 2015, 2020). To lyse the cells, 50 μL/well of ice-chilled 0.1 % nuclease-free bovine serum albumin (BSA) was added, and plates were vigorously vortexed on ice for 30 min. The lysates were centrifuged at 2000 g for 15 min, and the supernatants were either used immediately for qRT-PCR or stored at −80 °C until analysis.

Quantification of parasite and host nucleic acids was performed using a one-step qRT-PCR SYBR Green kit (HiScript II, Vazyme) on a StepOnePlus real-time PCR system (Applied Biosystems). Each 20 μL reaction contained 2.0 μL of diluted lysate (1:100 diluted for Cp18S and 1:2000 for Hs18S), 0.4 μL each of forward and reverse primers (10 μM), 1.0 μL enzyme mix, 0.4 μL ROX reference dye, 10 μL 2 × SYBR Green mix, and 5.8 μL RNase-free ddH_2O. *C. parvum* 18S rRNA was amplified using primers Cp18S-1011F (5′-TTG TTC CTT ACT CCT TCA GCA C-3′) and Cp18S-1185R (5′-TCC TTC CTA TGT CTG GAC CTG-3′), while host 18S rRNA was amplified using Hs18S-1F (5′-GGC GCC CCC TCG ATG CTC TTA-3′) and Hs18S-1R (5′-CCC CCG GCC GTC CTC TTA-3′). Thermal cycling parameters and melting curve analysis were as previously published (Zhang and Zhu, 2015, 2020).

Relative parasite growth was calculated using the $\Delta\Delta C_T$ method (Zhang and Zhu, 2015, 2020): first, ΔC_T values were obtained by subtracting $C_{T(Hs18S)}$ from $C_{T(Cp18S)}$ for each well, then $\Delta\Delta C_T$ values were calculated by comparing $\Delta C_{T(sample)}$ to the mean ΔC_T of vehicle controls. Percent inhibition was expressed as $1–2^{\wedge}(\Delta\Delta C_T) \times 100$ %. EC_{50} values were derived from dose–response curves fitted to a four-parameter logistic model using nonlinear regression.

2.5. Cytotoxicity assay

Cytotoxic effects of the compounds on HCT-8 cells were measured using a colorimetric MTS cell viability assay (Saint-Bio, Shanghai) (Li et al., 2025; Yang et al., 2023). Cells were seeded in 96-well plates at 5000 cells/well and allowed to attach for 16 h before treatment. Serially diluted compounds (final DMSO 0.5 %) in complete culture medium were added, and the plates were incubated for 41 h. After washing three times with PBS, 10 μL/well of MTS reagent was added, and plates were incubated for 2 h at 37 °C. Absorbance was measured at 490 nm using a Synergy LX multimode plate reader (BioTek). Cell viability was calculated relative to vehicle controls, and TC_{50} values were determined from the resulting dose–response curves. The selectivity index (SI) was calculated as TC_{50}/EC_{50}.

2.6. Effects of the top hit H1402 on the host cell morphology and parasite development

Based on the in vitro efficacy data, H1402 as one of the top hits was used to assess its effects on the morphology and *C. parvum* development in vitro. HCT-8 cell monolayers were cultured on poly-L-lysine coated coverslips placed in 48-well culture plates. Upon inoculation with *C. parvum* oocysts for 3 h, H1402 at 2.5 μM (~EC_{60} concentration) was added into the HCT-8 monolayers by a medium exchange as described

above. The vehicle (0.5 % DMSO) was used as negative control. The monolayers were allowed to grow for additional 8 h (= total 11 hpi), at which the majority of the parasites developed into multi-nucleus meronts near the end of the first cell cycle. The monolayers were fixed, immuno-labeled with fluorescein-labeled *Vicia villosa* lectin (VVL), counterstained with 4′,6-diamidino-2-phenylindole (DAPI), and examined under an Olympus BX53 fluorescence microscope as described (Wang et al., 2024a).

2.7. In vivo efficacy assay

Three top hits (H1402, YFM1, and YFM3) were evaluated in a chronic *C. tyzzeri* infection model in wild-type C57BL/6 mice as previously described (Fig. 2A) (Liu et al., 2023). Mice (6–8 weeks old, balanced for sex) were given DXP and TET in drinking water on alternating days starting 7 days before infection and continuing until the end of the experiment. Each mouse was orally inoculated with 1×10^5 oocysts of *C. tyzzeri* JLU01 strain on day 7 of treatment.

On day 10 post-infection (dpi), mice were randomly assigned to treatment groups and administered compounds by oral gavage once daily for 7 consecutive days. H1402 was given at 25 mg/kg/d, whereas YFM1 and YFM3 were given at 15 mg/kg/d. Paromomycin (1000 mg/kg/d) served as a positive control, and 5 % DMSO served as vehicle control. Each group included eight mice (four males and four females), while paromomycin group used six (three for each sex).

Mice were weighed daily and observed for general health. For each mouse, fecal pellets were collected individually on days 0, 1, 3, 5, and 7 post-administration (dpa; corresponding to 10–17 dpi). Feces were weighed, suspended in water (approximately 100 mg/mL), and stored at 4 °C. DNA was extracted from ~0.2 mL of fecal suspension after eight freeze–thaw cycles in lysis buffer, using the TIANamp Stool DNA Kit (Tiangen, Beijing).

Oocyst shedding was quantified by SYBR Green qPCR targeting the *C. tyzzeri* gene CTYZ_00001592 with primers Ctyz_1592F (5′-AGT GAT TCA GAT TAT TTA GAA GGT G-3′) and Ctyz_1592R (5′-TCA ATT CCT TCC AAA GGT TTT AC-3′) (Liu et al., 2023). Amplification consisted of an initial denaturation at 95 °C for 30 s, followed by 40 cycles of 95 °C for 5 s and 60 °C for 30 s, and a melting curve analysis at the end of cycling. Standard curves were established by spiking serially diluted oocysts (3.2×10^2 to 5×10^6 per sample) into negative mouse feces and processing them identically to experimental samples.

2.8. Statistical analysis

All in vitro assays were repeated at least twice independently, each including three or more biological replicates and two technical replicates for qRT-PCR. In vivo experiments used 10 mice per treatment group. Quantitative data were analyzed using GraphPad Prism v10. Group comparisons were made by two-way analysis of variance (ANOVA) followed by Dunnett's multiple-comparison tests as indicated in the figure legends or text.

3. Results

3.1. Cryptosporidium species used for in vitro and in vivo drug efficacy studies

This study used *C. parvum* for in vitro drug efficacy assay, and *C. tyzzeri* for in vivo drug testing. Since *C. tyzzeri* is a natural mouse parasite closely related to *C. parvum* and *C. hominis*, and able to establish chronic infection in chemically immunosuppressed wild-type mice, *C. tyzzeri* infection in mice provides a cost-effective model for evaluating anti-cryptosporidial drug efficacy (Liu et al., 2023). The *C. tyzzeri* model has been validated with paromomycin (1000 mg/kg/d) and nitazoxanide (100 mg/kg/d) for comparability to the *C. parvum* infection model in immuno-deficient mice (Liu et al., 2023). However, it is an alternative model, rather than a replacement of the *C. parvum* infection model, particularly for primary evaluation of in vivo anti-cryptosporidial drug efficacies. Drugs showing anti-*C. tyzzeri* activity in vivo can be further evaluated for anti-*C. parvum* and anti-*C. hominis* efficacies in small and large animal models.

3.2. Carbazole aminoalcohol compounds exhibit low-micromolar in vitro efficacy against C. parvum

In the primary screening, 36 CAA analogues were tested in a 44-h *C. parvum* infection assay at 5 μM and 2.5 μM, with parasite growth quantified by qRT-PCR. At 5 μM, growth inhibition ranged from 17.9 % (DLP1113) to 90.4 % (DLP1103), with a mean inhibition of 57.1 % across all compounds (Fig. 1C; Supplementary Table S1). At the lower concentration of 2.5 μM, nine compounds lost activity, producing negative inhibition values (−17.3 % to −1.5 %), while the remaining 27 compounds retained positive inhibition from 0.6 % to 79.0 % (mean 23.9 %).

Five compounds achieved >50 % inhibition at 2.5 μM (DLP1103, DLP1104, H1402, YFM1, and YFM3), all belonging to the mono- or di-halogenated carbazole cores (core 3 or core 4 derivatives). These five compounds, together with three additional analogues chosen for comparison, were subjected to dose–response analysis. All eight analogues demonstrated single-digit, low-micromolar EC_{50} values, ranging from 1.53 μM (DLP1103) to 6.86 μM (DLP1109) (mean EC_{50} = 3.18 μM) (Fig. 1E–Table 1).

Cytotoxicity against HCT-8 host cells was also assessed using the MTS assay. TC_{50} values ranged from 6.54 μM (DLP1103) to 15.36 μM (H1430), with a mean TC_{50} of 9.43 μM. These values correspond to selectivity indices ($SI = TC_{50}/EC_{50}$) between 1.66 (DLP1109) and 4.30 (DLP1103), indicating moderate cytotoxicity and relatively narrow therapeutic windows for this chemical class. Based on our previously published host–parasite selectivity model (Yang et al., 2023), these low SI values suggest that part of the observed in vitro anti-cryptosporidial activity may result from off-target effects on host cells rather than purely parasite-specific inhibition.

3.3. Three top hits reduce oocyst shedding in a mouse model of chronic C. tyzzeri infection

Based on their in vitro potency, three core 4 analogues, H1402, YFM1, and YFM3, were selected for in vivo evaluation. These compounds have EC_{50} values of 2.35, 2.58, and 2.06 μM, respectively, and represent structural variants with either linear (H1402) or branched (YFM1, YFM3) three- or four-carbon side chains (Fig. 1E).

In the chronic *C. tyzzeri* mouse model, untreated controls (vehicle) exhibited a progressive increase in oocyst shedding over the 7-day observation period, with an average increase to 247.5 % relative to baseline (266.4 % in females and 222.3 % in males) (Fig. 2B and C). In contrast, all three CAA treatments significantly suppressed oocyst shedding in a time-dependent manner (Fig. 2D, Fig. S2). On day 5 post-administration (dpa), mean reductions relative to baseline were 55.9 % for H1402 (56.8 % in males, 54.9 % in females), 56.7 % for YFM1 (both sexes), and 58.1 % for YFM3 (61.0 % in males, 55.2 % in females). Reductions remained significant on day 7 dpa, with final parasite loads reduced by 55.9 %–58.1 % compared with the marked increase in the vehicle group ($P < 0.01$ by Dunnett's test) (Table 1).

For comparison, paromomycin (1000 mg/kg/d) achieved an 84.2 % reduction in oocyst shedding under the same experimental conditions, consistent with prior studies using this model (Liu et al., 2023). These data confirm that although CAA analogues are less potent than paromomycin, they still achieve meaningful suppression of parasite burden in vivo at relatively moderate oral doses.

Treatment with H1402, YFM1, or YFM3 was generally well tolerated. No overt signs of toxicity or distress were observed during daily monitoring. Body weight analysis showed that vehicle-treated mice gained a

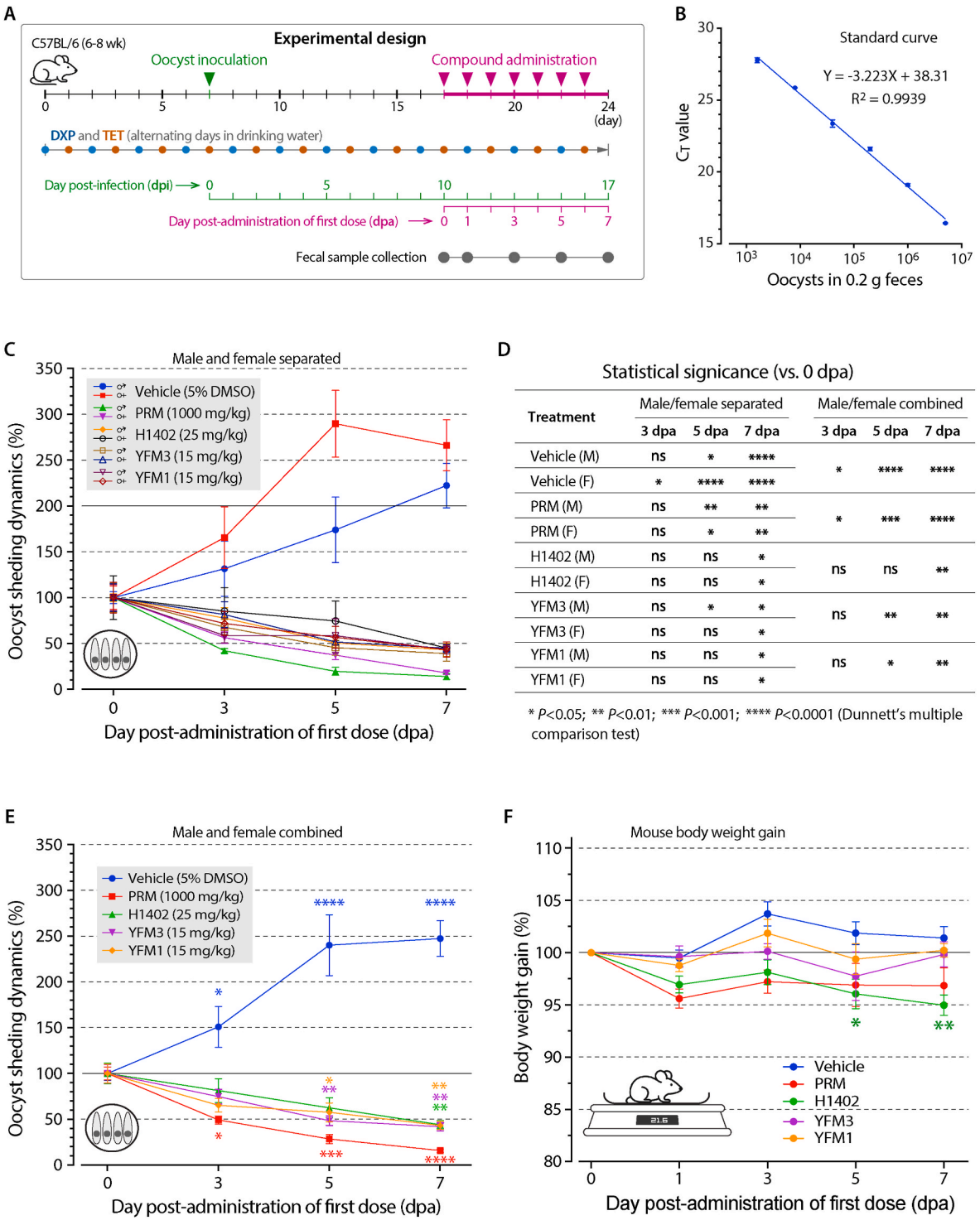

Treatment	Male/female separated			Male/female combined		
	3 dpa	5 dpa	7 dpa	3 dpa	5 dpa	7 dpa
Vehicle (M)	ns	*	****	*	****	****
Vehicle (F)	*	****	****			
PRM (M)	ns	**	**	*	***	****
PRM (F)	ns	*	**			
H1402 (M)	ns	ns	*	ns	ns	**
H1402 (F)	ns	ns	*			
YFM3 (M)	ns	*	*	ns	**	**
YFM3 (F)	ns	ns	*			
YFM1 (M)	ns	ns	*	ns	*	**
YFM1 (F)	ns	ns	*			

* $P<0.05$; ** $P<0.01$; *** $P<0.001$; **** $P<0.0001$ (Dunnett's multiple comparison test)

Fig. 2. In vivo efficacy of three top CAAs in a chronic *Cryptosporidium tyzzeri* mouse model. (A) Experimental design: C57BL/6 mice were treated with dexamethasone phosphate (DXP) and tetracycline (TET) in alternating days starting 7 days before infection, orally infected with 10^5 *C. tyzzeri* oocysts, and then treated with CAAs or controls for 7 days starting at day 10 post-infection. **(B)** Standard curve was established by spiking serially diluted *C. parvum* oocysts into negative mouse feces, followed by the extraction of stool DNA and detection of *C. parvum* DNA by qPCR as described in the Materials and Methods. **(C–E)** Oocyst shedding dynamics in mice treated with H1402 (25 mg/kg/day), YFM1 (15 mg/kg/day), or YFM3 (15 mg/kg/day) compared with vehicle (5 % DMSO) and paromomycin (1000 mg/kg/day) controls. Data are separated by sex (C) and for mixed sexes (E) with statistical significances summarized in table (D). **(F)** Body-weight changes during treatment, expressed as percentage change relative to day 0. Data are means ± SEM for 10 mice per group (5 male and 5 female). Statistical significance was determined by two-way ANOVA followed by Dunnett's multiple-comparison test (*$P < 0.05$; **$P < 0.01$; ***$P < 0.001$; ****$P < 0.0001$ vs. day 0).

Table 1
Summary of in vitro and in vivo anti-cryptosporidial efficacies of selected carbazole aminoalcohols (CAAs).

No. [a]	Name	Mol Wt.	In vitro on *C. parvum* [b]			In vivo on *C. tyzzeri* (7 dpa vs. 0 dpa) [c]			
			EC_{50} (μM)	TC_{50} (μM)	SI	Dose/day	Oocysts (%)	N	P-value
n/a	Vehicle	N/A	N/A	N/A	N/A	–	247.47 ± 19.58	7	<0.0001
n/a	Paromomycin [d]	713.71	123.4	>1000	>8.1	1000 mg/kg	15.82 ± 1.88	6	<0.0001
18	H1402	350.10	2.35	7.32	3.11	25 mg/kg	44.11 ± 4.59	8	<0.01
29	YFM1	364.11	2.58	6.93	2.69	15 mg/kg	43.32 ± 4.42	8	<0.01
30	YFM3	364.11	2.06	8.13	3.94	15 mg/kg	41.9 ± 4.49	8	<0.01
3	DLP1108	310.20	4.15	12.43	3	N/T	–	–	–
4	DLP1109	324.22	6.86	11.4	1.66	N/T	–	–	–
15	DLP1103	344.17	1.53	6.54	4.3	N/T	–	–	–
16	DLP1104	358.18	2.2	7.33	3.3	N/T	–	–	–
28	H1430	364.11	3.73	15.36	4.11	N/A	–	–	–

[a] No. refers to the compound number listed in the Supplementary Table S1.
[b] EC_{50}, half-maximal effective concentration from 44-h *C. parvum* growth inhibition assay (qRT-PCR); TC_{50}, half-maximal cytotoxic concentration in HCT-8 cells (MTS assay); SI, selectivity index (TC_{50}/EC_{50}).
[c] In vivo data show relative parasite loads in fecal samples collected at day 7 post-administration (dpa), normalized to baseline (day 0). Data are mean ± SEM. Statistical significance was determined by two-way ANOVA followed by Dunnett's test compared with vehicle control. N/T, not tested in vivo; N/A, not applicable.
[d] In vitro data on paromomycin are derived from one of our previous studies (Zhang and Zhu, 2015).

small amount of weight (1.4 %) over the 7-day period, whereas paromomycin-treated mice lost 3.2 % of body weight on average. Weight changes were minimal in YFM1-and YFM3-treated mice (0.2 % loss), but slightly greater in H1402-treated mice (5.0 % loss), which reached statistical significance on days 5 and 7 dpa ($P < 0.05$ and $P < 0.01$, respectively) (Fig. 2F). Overall, the data suggest that the three lead CAAs have acceptable tolerability profiles in this model at the doses tested.

3.4. The carbazole aminoalcohol H1402 displays a parasititstatic effect on *C. parvum* in vitro

We microscopically examined the effect of H1402, a representative CAA compound, on the intracellular development of *C. parvum*. HCT-8 cell monolayers were infected by incubation with *C. parvum* oocysts for 3 h, followed by treatment with H1402 at 2.5 μM (~EC_{60}) for 8 h, with 1.0 % DMSO serving as the negative control. At this time point, no apparent morphological differences were observed in host cell monolayers between the control and H1402-treated groups (Fig. 3A).

In the negative control group, most intracellular parasites progressed to the end of the first merogonic cycle and developed into multinucleated meronts (approximately 4–6 μm in size) (Fig. 3B, left; Fig. 3C). In contrast, in the H1402-treated group, virtually all parasites remained as single-nucleus trophozoites (approximately 2.0–2.5 μm in size), indicating a stage-specific developmental arrest (Fig. 3B, right; Fig. 3C). Notably, although H1402 treatment arrested parasite development, it only slightly and not significantly reduced the total number of intracellular parasites (Fig. 3C). Together, these data indicate that H1402 exerts a parasititstatic, rather than parasiticidal, effect on *C. parvum* in vitro.

Overall, these results demonstrate that CAAs display reproducible, low-micromolar inhibition of *C. parvum* growth in vitro, and three analogues with dichlorinated carbazole attached with linear or branched short side chains achieve moderate, statistically significant reduction of *C. tyzzeri* oocyst shedding in vivo. H1402, one of the top CAA hits, exhibits parasititstatic effect on the in vitro growth of *C. parvum*. The observed efficacy, combined with acceptable tolerability, supports further optimization of this chemical scaffold to improve potency, selectivity, and safety.

4. Discussion

Carbazole aminoalcohol (CAA) analogues were initially explored for antimalarial activity. The first lead compound, TDR30137, is a dihalogenated carbazole containing a bulky bicyclic amine substituent, which inhibited the chloroquine-resistant *Plasmodium falciparum* K1 strain with an EC_{50} of 57 nM in human erythrocytes but was ineffective against *P. berghei* in vivo in mice (Supplementary Fig. S3) (Molette et al., 2013). Subsequent structural simplification at the amine moiety to single- or double-ring substituents not only improved in vitro potency (EC_{50} of 9–16 nM for compounds 12 and 13a) but also restored in vivo efficacy against *P. berghei* at 100 mg/kg/day for four days. Similarly, JFD03612SC, a dichlorinated carbazole bearing a four-carbon ring substituent, displayed dual activity against *Schistosoma japonicum* adult worms (10 μg/mL) and *P. falciparum* 3D7 parasites (EC_{50} = 2.67 μM) (Wang et al., 2017b).

Our data extend these findings to *Cryptosporidium*, representing, to our knowledge, the first systematic evaluation of CAAs against this genus. We observed that dihalogenation of the carbazole core (core 4) together with short linear or branched aminoalcohol side chains was generally associated with improved anti-cryptosporidial activity. This is consistent with the electronic and steric effects described in earlier SAR studies (Molette et al., 2013; Wang et al., 2016a), where halogen substitution increases electron density and lipophilicity of the aromatic core, potentially enhancing membrane permeability and interaction with hydrophobic binding sites. Interestingly, while antimalarial activity was reported to improve with increasing side-chain length (from 3C to 8C linear chains), our results suggest that relatively short side chains may be more favorable for anti-cryptosporidial activity, possibly reflecting differences in parasite membrane environment, uptake mechanisms, or target binding sites (Supplementary Fig. S4).

Among the CAAs tested, H1402 stood out as a particularly consistent performer, showing low-micromolar or high-nanomolar efficacy not only against *Cryptosporidium* but also against *Plasmodium*, *Trypanosoma*, and *Echinococcus* spp. across multiple studies (Dang et al., 2018; Liu et al., 2018; Wang et al., 2017a, 2017b). The relatively narrow selectivity indices observed for H1402 (SI ≈ 3) and other hits indicate that host-cell effects contribute to their in vitro activity, which is not uncommon for lipophilic scaffolds that partition into host membranes. Given the amphiphilic nature of CAAs, i.e., a planar, lipophilic carbazole core linked to a polar, hydrogen-bonding aminoalcohol, these compounds are likely to accumulate in lipid bilayers, where they may perturb membrane-associated processes or access multiple intracellular targets. However, based on available data and the absence of overt cytotoxicity at effective doses in vivo, a detergent-like nonspecific mechanism is unlikely. Rather, the activity profile is more consistent with weak-to-moderate binding to one or more parasite targets, potentially combined with secondary effects on host cell pathways.

Previous studies have shown that H1402 can inhibit mammalian DNA topoisomerase I (Topo I), with detectable activity in a DNA Topo I

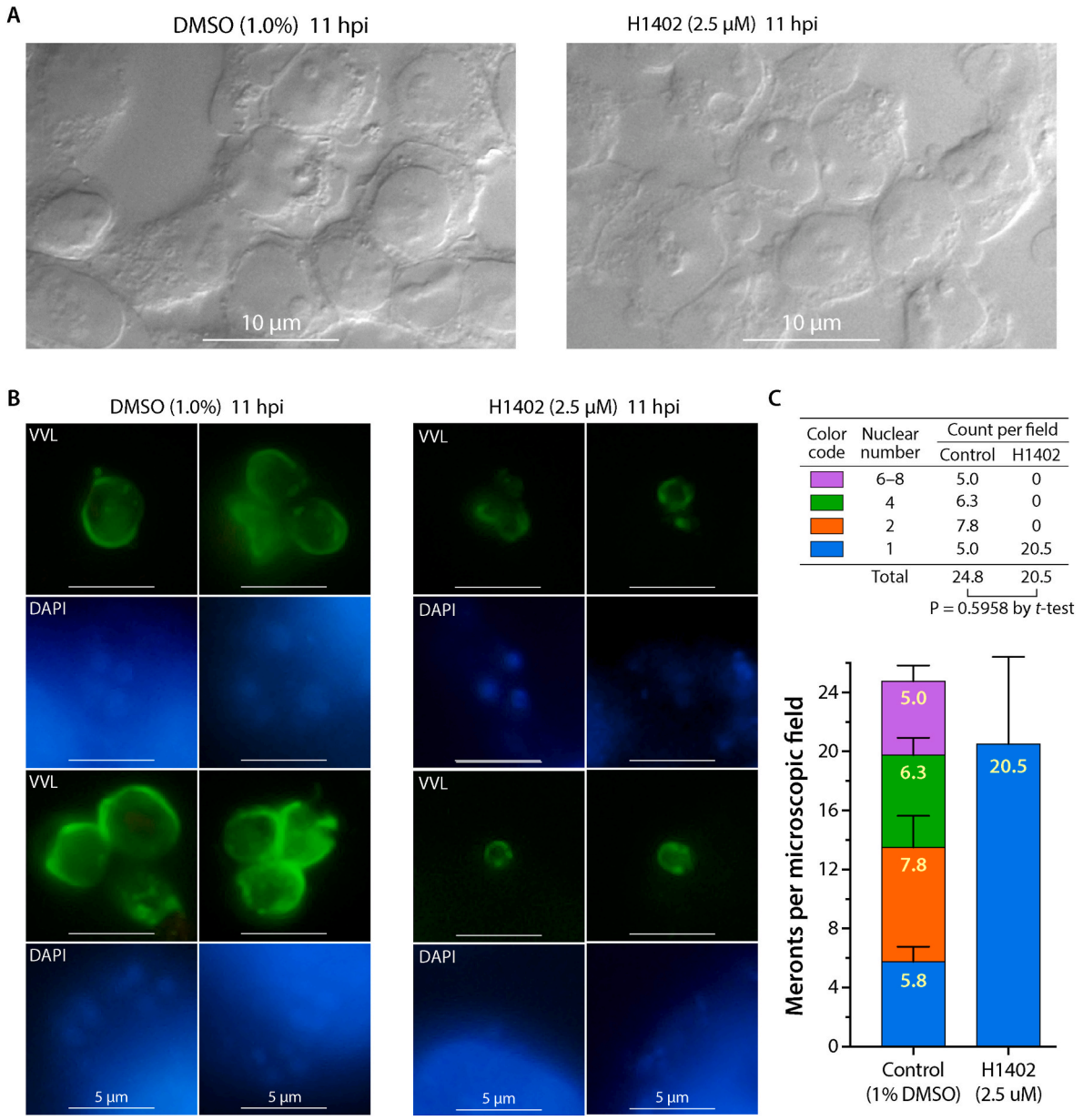

Fig. 3. Effects of H1402 on host cell monolayers and development during the first merogonic cell cycle of *Cryptosporidium parvum* in vitro. HCT-8 monolayers were incubated *C. parvum* oocysts for 3 h to allow excystation and sporozoite invasion, followed by treatment with H1402 (2.5 µM; ~EC_{60}) for 8 h. Cells were then fixed and subjected to immunofluorescence labeling. **(A)** H1402 treatment had no apparent effect on the morphology or integrity of HCT-8 cell monolayers. **(B)** In the negative control (1.0 % DMSO; left), intracellular parasites progressed through the first merogonic cycle and developed into multinucleated meronts. In contrast, H1402 treatment resulted in a stage-specific developmental arrest, with all intracellular parasites remaining as single-nucleus trophozoites (right). **(C)** Although H1402 treatment arrested parasite development, it did not significantly reduced the total number of intracellular parasites (P = 0.5958, two-tailed Student's *t*-test; n = 30 microscopic field).

assay at concentrations ≥50 µM, and can arrest HeLa cell growth at the G_2 phase at concentrations ≥20 µM (Wang et al., 2016b). H1402 has also been reported to interfere with β-hematin formation in *P. falciparum* (IC_{50} = 151.5 µM) (Wang et al., 2017b), whereas other carbazole aminoalcohol (CAA) analogues were shown to interact with *P. falciparum* Hsp90, with dissociation constants in the mid-micromolar range (K_d = 25.6 and 28.1 µM for compounds 3B and 5B, respectively) (Wang et al., 2016a).

In the present study, however, H1402 induced a pronounced stage-specific developmental arrest of *C. parvum* at the trophozoite stage at a substantially lower concentration (2.5 µM; Fig. 3), suggesting that one or more parasite targets may be engaged with higher apparent potency in *Cryptosporidium*. Given the essential role of DNA replication and chromatin dynamics during the trophozoite-to-meront transition, parasite DNA topoisomerases, particularly Topo I, represent plausible candidate targets. The *C. parvum* genome encodes a single Topo I ortholog (CpTopo1; gene ID cgd7_3350), as well as several additional DNA topoisomerases. CpTopo1 shares approximately 40 % amino acid sequence identity with human Topo I (UniProt ID P11387), suggesting both evolutionary conservation and the potential for exploitable structural divergence. If CpTopo1 is confirmed as a molecular target of H1402, this would provide a rational basis for structure-guided lead optimization aimed at improving parasite selectivity and reducing host activity. Such optimized compounds could serve not only as candidate therapeutics but also as chemical probes to investigate the biological functions of Topo I during *C. parvum* intracellular development.

Importantly, the three top hits (H1402, YFM1, YFM3) significantly reduced oocyst shedding in a chronic *C. tyzzeri* mouse model, achieving 56–58 % reduction at relatively moderate oral doses. This efficacy is lower than that of paromomycin but the administrated doses were also much lower (i.e., 25 mg/kg/d for H1402 and 15 mg/kg/d for YFM1 and YFM3; vs. 1000 mg/kg/d for paromomycin), which is noteworthy given the chemical novelty and lack of prior optimization for *Cryptosporidium*. Moreover, the good tolerability of these compounds in mice, despite the moderate cytotoxicity observed in vitro, suggests a reasonable therapeutic window that may be widened through medicinal chemistry optimization, for example, by fine-tuning lipophilicity (cLogP) or polar surface area to balance cell permeability with selectivity.

Overall, our findings position CAAs as promising lead scaffolds for anti-cryptosporidial drug development. Future studies should prioritize systematic structure–activity relationship (SAR) optimization, guided by physicochemical parameters such as lipophilicity (logP), aqueous solubility, and metabolic stability. Parallel pharmacokinetic/pharmacodynamic (PK/PD) studies will be needed to better correlate exposure with efficacy and to determine whether higher oral doses or alternative formulations could enhance therapeutic benefit. Combination studies with standard-of-care drugs, such as nitazoxanide or paromomycin, may also be valuable to assess potential synergy and reduce the risk of resistance emergence.

In summary, this study provides the first comprehensive evaluation of carbazole aminoalcohols against *Cryptosporidium* spp., demonstrating low-micromolar in vitro activity and significant in vivo efficacy in a murine model. These results expand the antiparasitic spectrum of CAAs and support their further optimization as leads for the development of novel anti-cryptosporidial therapeutics.

CRediT authorship contribution statement

Mingxiao Liu: Writing – original draft, Visualization, Methodology, Investigation, Formal analysis. **Weisi Wang:** Resources, Investigation. **Qi Zheng:** Resources, Investigation. **Di Zhang:** Investigation. **Dongqiang Wang:** Investigation. **Chenchen Wang:** Investigation. **Jigang Yin:** Writing – review & editing, Supervision, Funding acquisition. **Liping Duan:** Writing – review & editing, Validation, Supervision, Resources, Conceptualization. **Guan Zhu:** Writing – review & editing, Visualization, Validation, Supervision, Project administration, Methodology, Funding acquisition, Formal analysis.

Conflict of interest

The authors declare no conflict of interest.

Acknowledgements

This research was supported by grants of the National Key Research and Development Program of China (2022YFD1800200 to G.Z.), and the National Natural Science Foundation of China (82473743 to W.W.). We thank Assoc. Prof. Zhuo Chen for performing NMR and HRMS analyses.

Appendix A. Supplementary data

Supplementary data to this article can be found online at https://doi.org/10.1016/j.ijpddr.2026.100631.

References

Cai, X.L., Wang, W., Lai, D.H., Zhang, X., Yao, J., Yu, Y., Li, S., Hide, G., Bai, H., Duan, L., Lun, Z.R., 2021. Identification of an orally active carbazole aminoalcohol derivative with broad-spectrum anti-animal trypanosomiasis activity. Acta Trop. 219, 105919.

Checkley, W., White Jr., A.C., Jaganath, D., Arrowood, M.J., Chalmers, R.M., Chen, X.M., Fayer, R., Griffiths, J.K., Guerrant, R.L., Hedstrom, L., Huston, C.D., Kotloff, K.L., Kang, G., Mead, J.R., Miller, M., Petri Jr., W.A., Priest, J.W., Roos, D.S., Striepen, B., Thompson, R.C., Ward, H.D., Van Voorhis, W.A., Xiao, L., Zhu, G., Houpt, E.R., 2015. A review of the global burden, novel diagnostics, therapeutics, and vaccine targets for cryptosporidium. Lancet Infect. Dis. 15, 85–94.

Dang, Z., Xu, S., Zhang, H., Gui, W., Zhao, Y., Duan, L., Hu, W., 2018. In vitro and in vivo efficacies of carbazole aminoalcohols in the treatment of alveolar echinococcosis. Acta Trop. 185, 138–143.

Khan, S.M., Witola, W.H., 2023. Past, current, and potential treatments for cryptosporidiosis in humans and farm animals: a comprehensive review. Front. Cell. Infect. Microbiol. 13, 1115522.

Kotloff, K.L., Nataro, J.P., Blackwelder, W.C., Nasrin, D., Farag, T.H., Panchalingam, S., Wu, Y., Sow, S.O., Sur, D., Breiman, R.F., Faruque, A.S., Zaidi, A.K., Saha, D., Alonso, P.L., Tamboura, B., Sanogo, D., Onwuchekwa, U., Manna, B., Ramamurthy, T., Kanungo, S., Ochieng, J.B., Omore, R., Oundo, J.O., Hossain, A., Das, S.K., Ahmed, S., Qureshi, S., Quadri, F., Adegbola, R.A., Antonio, M., Hossain, M.J., Akinsola, A., Mandomando, I., Nhampossa, T., Acacio, S., Biswas, K., O'Reilly, C.E., Mintz, E.D., Berkeley, L.Y., Muhsen, K., Sommerfelt, H., Robins-Browne, R.M., Levine, M.M., 2013. Burden and aetiology of diarrhoeal disease in infants and young children in developing countries (the Global Enteric Multicenter Study, GEMS): a prospective, case-control study. Lancet 382, 209–222.

Levine, M.M., Nasrin, D., Acacio, S., Bassat, Q., Powell, H., Tennant, S.M., Sow, S.O., Sur, D., Zaidi, A.K.M., Faruque, A.S.G., Hossain, M.J., Alonso, P.L., Breiman, R.F., O'Reilly, C.E., Mintz, E.D., Omore, R., Ochieng, J.B., Oundo, J.O., Tamboura, B., Sanogo, D., Onwuchekwa, U., Manna, B., Ramamurthy, T., Kanungo, S., Ahmed, S., Qureshi, S., Quadri, F., Hossain, A., Das, S.K., Antonio, M., Saha, D., Mandomando, I., Blackwelder, W.C., Farag, T., Wu, Y., Houpt, E.R., Verweiij, J.J., Sommerfelt, H., Nataro, J.P., Robins-Browne, R.M., Kotloff, K.L., 2020. Diarrhoeal disease and subsequent risk of death in infants and children residing in low-income and middle-income countries: analysis of the GEMS case-control study and 12-month GEMS-1A follow-on study. Lancet Glob Health 8, e204–e214.

Li, M., Yin, J., Wang, D., Zou, B., Zhu, G., 2025. Targeting translation initiation yields fast-killing therapeutics against the zoonotic parasite *Cryptosporidium parvum*. PLoS Pathog. 21, e1012881.

Liu, C., Yin, J., Xue, J., Tao, Y., Hu, W., Zhang, H., 2018. In vitro effects of amino alcohols on *Echinococcus granulosus*. Acta Trop. 182, 285–290.

Liu, M., Zhang, D., Wang, D., Wu, X., Zhang, Y., Yin, J., Zhu, G., 2023. Cost-effective in vivo and in vitro mouse models for evaluating anticryptosporidial drug efficacy: assessing vorinostat, docetaxel, and Baicalein. J. Infect. Dis. 228, 1430–1440.

Love, M.S., Choy, R.K.M., 2021. Emerging treatment options for cryptosporidiosis. Curr. Opin. Infect. Dis. 34, 455–462.

Molette, J., Routier, J., Abla, N., Besson, D., Bombrun, A., Brun, R., Burt, H., Georgi, K., Kaiser, M., Nwaka, S., Muzerelle, M., Scheer, A., 2013. Identification and optimization of an aminoalcohol-carbazole series with antimalarial properties. ACS Med. Chem. Lett. 4, 1037–1041.

Roblin, M., Canniere, E., Barbier, A., Daandels, Y., Dellevoet-Groenewegen, M., Pinto, P., Tsaousis, A., Leruste, H., Brainard, J., Hunter, P.R., Follet, J., 2023. Study of the economic impact of cryptosporidiosis in calves after implementing good practices to manage the disease on dairy farms in Belgium, France, and the Netherlands. Curr Res Parasitol Vector Borne Dis 4, 100149.

Schneider, A., Wendt, S., Lubbert, C., Trawinski, H., 2021. Current pharmacotherapy of cryptosporidiosis: an update of the state-of-the-art. Expert Opin Pharmacother 22, 2337–2342.

Shaw, H.J., Innes, E.A., Morrison, L.J., Katzer, F., Wells, B., 2020. Long-term production effects of clinical cryptosporidiosis in neonatal calves. Int. J. Parasitol. 50, 371–376.

Smith, C.D., Wang, A., Vembaiyan, K., Zhang, J., Xie, C., Zhou, Q., Wu, G., Chen, S.R., Back, T.G., 2013. Novel carvedilol analogues that suppress store-overload-induced Ca2+ release. J. Med. Chem. 56, 8626–8655.

Wang, D., Jiang, P., Wu, X., Zhang, Y., Wang, C., Li, M., Liu, M., Yin, J., Zhu, G., 2024a. Requirement of microtubules for secretion of a micronemal protein CpTSP4 in the invasive stage of the apicomplexan *Cryptosporidium parvum*. mBio 15, e0315823.

Wang, D., Jiang, P., Yang, X., Zhang, J., Chen, T., Hu, M., Caccio, S.M., Yin, J., Zhu, G., 2024b. Novel strategy to quantify the viability of oocysts of *Cryptosporidium parvum* and *C. hominis*, a risk factor of the waterborne protozoan pathogens of public health concern. Water Res. 258, 121788.

Wang, T., Mäser, P., Picard, D., 2016a. Inhibition of *Plasmodium falciparum* Hsp90 contributes to the antimalarial activities of aminoalcohol-carbazoles. J. Med. Chem. 59, 6344–6352.

Wang, W., Li, J., Yao, J., Wang, T., Li, S., Zheng, X., Duan, L., Zhang, W., 2017a. In vitro and in vivo efficacies of novel carbazole aminoalcohols in the treatment of cystic echinococcosis. J. Antimicrob. Chemother. 72, 3122–3130.

Wang, W., Li, Q., Wei, Y., Xue, J., Sun, X., Yu, Y., Chen, Z., Li, S., Duan, L., 2017b. Novel carbazole aminoalcohols as inhibitors of β-hematin formation: antiplasmodial and antischistosomal activities. Int J Parasitol Drugs Drug Resist 7, 191–199.

Wang, W., Sun, X., Sun, D., Li, S., Yu, Y., Yang, T., Yao, J., Chen, Z., Duan, L., 2016b. Carbazole aminoalcohols induce antiproliferation and apoptosis of human tumor cells by inhibiting topoisomerase I. ChemMedChem 11, 2675–2681.

Yang, B., Yan, Y., Wang, D., Zhang, Y., Yin, J., Zhu, G., 2023. On-target inhibition of *Cryptosporidium parvum* by nitazoxanide (NTZ) and paclitaxel (PTX) validated using a novel MDR1-transgenic host cell model and algorithms to quantify the effect on the parasite target. PLoS Negl Trop Dis 17, e0011217.

Zhang, H., Zhu, G., 2015. Quantitative RT-PCR assay for high-throughput screening (HTS) of drugs against the growth of *Cryptosporidium parvum* in vitro. Front. Microbiol. 6, 991.

Zhang, H., Zhu, G., 2020. High-Throughput screening of drugs against the growth of *Cryptosporidium parvum* in vitro by qRT-PCR. Methods Mol. Biol. 2052, 319–334.